

Variability of the FeK line relativistic component in a sample of Seyfert 1 galaxies

B. De Marco¹, M. Cappi², M. Dadina², G. G. C. Palumbo³

1-S.I.S.S.A., Trieste, Italy; 2-INAf, Bologna, Italy; 3-Bologna University, Bologna, Italy



Abstract

We present the analysis of X-ray spectral variability made on a sample of 7 Seyfert 1 bright galaxies, using XMM-Newton data. From the (XSA) public archive, we selected those bright Seyfert 1 showing one or more prominent flares in their 2-10 keV light curves. For each of them we extracted spectra in 3 different time intervals: before, during and after the flare. We fitted them with a simple power law and then shifted a narrow Gaussian emission and absorption line template across the 2.5-10 keV data, in order to investigate the presence of line-like features with a confidence level greater than 99%. Some highly significant features were detected in 3 out of 7 sources studied. In particular, the 3 sources showed the presence of a variable emission feature in the 4.5-5.8 keV band, characterized by an increase of its intensity after the flare peak. Because of the observed variability pattern, this feature seems to be ascribable to a reverberated redshifted relativistic component of the FeK line.

Selection of the sample

- Cross-correlation between the "XMM-Newton Master Log & Public Archive" (public data up to December 2004) and the "Véron Quasars and AGNs" catalog → selection of Seyfert 1, 1.2 and 1.5;
- Cross-correlation with the "ROSAT All Sky Survey: Bright Sources" catalog
 - selection of sources with ROSAT count rate >0.40 c/s
 - selection of observations with XMM-Newton exposure time >10 ks
- Definition of "flare": $\Delta CR = (CR_{max} - CR_{min}) / \langle CR \rangle \geq 0.5$, where $\langle CR \rangle$ = average count rate → selection of observations showing at least one flare in their EPIC pn light curves (the MCG 6-30-15 and MKN 766 observations as well as one observation of NGC 4051 were excluded because they are characterized by the superposition of a large number of flares, making hard to identify each of them).

name	flare	Δt (ks)	$\Delta CR_{(2-10 \text{ keV})}$
NGC 3783	I	52	0.65
	II	80	0.81
PG1211+143	I	12	1.00
TON 5 180	I	6	0.90
	II	9	0.60
NGC 4051	I	6	1.58
	II	8	0.88
I ZW 1	I	6	1.00
PG1448+273	I	4	0.61
AKN 564	I	2	1.09

Spectral analysis

The 2.5-10 keV spectra were extracted before, during and after each flare. A narrow Gaussian emission/absorption line template was added to the simple power law model and shifted along the entire energy band computing the χ^2 variations in order to search for line-like features with a confidence level >99%.

Results → 3 out of the 7 sources show highly significant emission and absorption features → PG1211+143, NGC 4051 and NGC 3783
 A variable emission feature was detected in the spectra of the 3 sources at rest energies of 4.5-5.8 keV. It is characterized by an increase of intensity in the periods following the flare peak. The variability of the feature is detected with a confidence level greater than 99%.

PG 1211+143 (z=0.081)

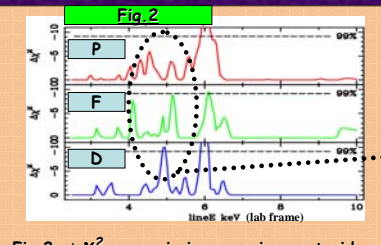
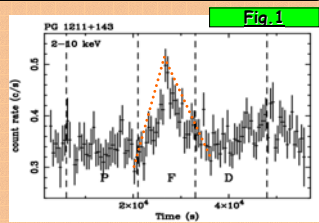


Fig. 2: $\Delta \chi^2$ vs. emission gaussian centroid-energy plot. The χ^2 variations are computed with respect to a "power law" model;

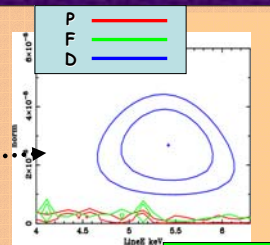
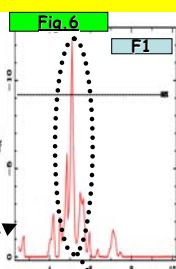
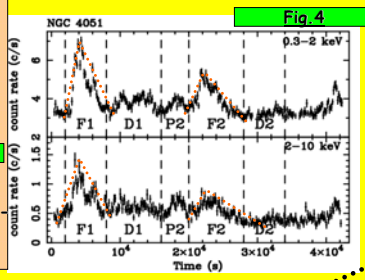


Fig. 3: Comparison between the normalization vs. gaussian centroid-energy contour plots (90% and 99%) in the 3 time intervals.

NGC 4051 (z=0.002)



NGC 3783 (z=0.01)

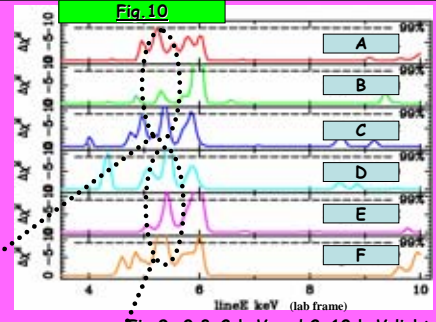
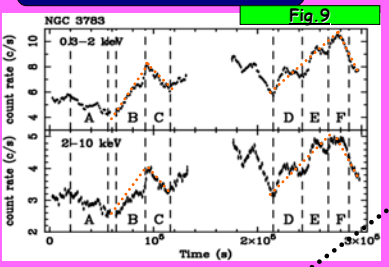


Fig. 9: 0.3-2 keV and 2-10 keV light curves with the chosen time intervals. The dotted red lines show the flares;

Fig. 10: $\Delta \chi^2$ vs. emission gaussian centroid-energy plot. The χ^2 variations are computed with respect to a "power law+emission gaussian (at E_obs ~ 6.3 keV)+emission gaussian (at E_obs ~ 6.9 keV)" model;

Fig. 11, 12: Comparison between the normalization vs. gaussian centroid-energy contour plots (90% and 99%) in the 6 time intervals.

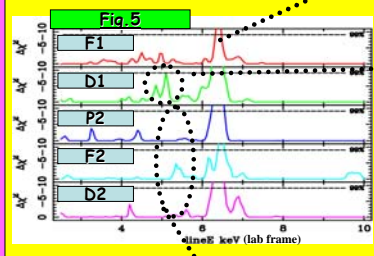


Fig. 5: $\Delta \chi^2$ vs. emission gaussian centroid-energy plot. The χ^2 variations are computed with respect to a "power law" model;

Fig. 6: Increase of significance of the feature at E_obs ~ 5 keV after the addition of an emission gaussian at E_obs ~ 6.4 keV;

Fig. 7, 8: Comparison between the normalization vs. gaussian centroid-energy contour plots (90% and 99%) in the 5 time intervals.

Conclusions: The observed variable emission feature ($E_{rest} \sim 4.5-5.8 \text{ keV}$) can be best interpreted as a highly redshifted component of the Fe K α line, produced in the innermost regions of the accretion disk. The variability pattern suggests that the line may be the product of hard X-ray flux continuum reverberation.